A ROLLER SEISMIC ISOLATION BEARING FOR HIGHWAY BRIDGES

George C. Lee[1], Yu-Chen Ou[2], Jianwei Song[3], Tiecheng Niu[4] and Zach Liang[5]

[1] *Professor, Department of Civil, Structural and Environmental Engineering, University at Buffalo, SUNY, Buffalo, U.S.A. E-mail: gclee@buffalo.edu.*

[2] *Assistant Professor, Department of Construction Engineering, Taiwan University of Science and Technology, Taipei, Chinese Taiwan. E-mail: yuchenou@mail.ntust.edu.tw*

[3] *Senior Research Scientist, Department of Civil, Structural and Environmental Engineering, University at Buffalo, SUNY, Buffalo, U.S.A. E-mail: songj@buffalo.edu.*

[4] *Visiting Professor, Department of Civil, Structural and Environmental Engineering, University at Buffalo, SUNY, Buffalo, U.S.A. E-mail: tiechengn@yahoo.com.*

[5] *Research Associate Professor, Department of Mechanical and Aerospace Engineering, University at Buffalo, SUNY, Buffalo, U.S.A. E-mail: zliang@buffalo.edu.*

ABSTRACT :
A new roller seismic isolation bearing is developed for use in highway bridges. This new bearing uses rolling of cylindrical rollers on V-shaped sloping surfaces to achieve seismic isolation. The bearing is characterized by a constant spectral acceleration under horizontal ground motions and by a self-centering capability, which are two desirable properties for seismic applications. The former makes resonance less likely to occur between the bearing and horizontal earthquakes while the latter guarantees the bridge superstructure can self-center to its original position after earthquakes. To provide supplemental energy dissipation to reduce the seismic responses, the bearing is designed with built-in sliding friction mechanisms. This paper first presents the acceleration responses of and forces acting on the bearing under base excitation. Next, the governing equation of horizontal motions, the base shear-horizontal displacement relationship, and conditions for self-centering for the rollers to maintain in contact with the bearing plates and for rolling without sliding are discussed.

KEYWORDS:
Seismic, Bridges, Bearings, Seismic isolation.

1. INTRODUCTION

Currently in the United States, there are two common types of seismic isolation bearings, elastomeric and sliding (Naeim and Kelly, 1999; Constantinou et al., 2007). Typical elastomeric bearings include low and high damping rubber bearings and lead-rubber bearings. These bearings achieve seismic isolation by the low shear stiffness of the elastomers. By using elastomers with a special compound, high damping rubber bearings can achieve higher inherent damping than low damping rubber bearings. In lead-rubber bearings, supplemental energy dissipation is realized by yielding of the lead core. Typical sliding bearings are concave sliding bearings (e.g., the Friction Pendulum bearing, EPS 2008) and flat sliding bearings (e.g., the EradiQuake bearing, R. J. Watson, Inc. 2008). In sliding bearings, seismic isolation is achieved by sliding actions. Supplemental energy dissipation is provided by sliding friction between contact surfaces.

Here, a new type of bearing called a roller seismic isolation bearing is developed for use in highway bridges (Lee et al., 2005). The bearing utilizes rolling of cylindrical rollers to achieve seismic isolation and exhibits three distinct characteristics. First, it has a zero post-elastic stiffness under a horizontal earthquake. This means that the spectral acceleration response of the bearing is independent of the magnitude and frequency content of the horizontal earthquake. Second, it is able to self-center to its initial position after an earthquake ends. Third, sliding friction mechanisms are integrated into the bearing to provide supplemental energy dissipation to reduce the displacement responses.

Figure 1 shows a simplified schematic view of the bearing. It consists of two rollers for bi-directional seismic isolation. Each roller is sandwiched between two bearing plates. The intermediate bearing plate has V-shaped sloping surfaces at the top and underside of the plate with the directions of the valleys of the two surfaces perpendicular to each other. The upper and lower bearing plates have flat surfaces in contact with the rollers. The upper plate is secured to the bridge superstructure and the lower plate mounted on the pier cap or abutment. Each bearing has two pairs of friction plates. Each pair corresponds to one of the principal directions of the bearing (rolling direction of individual roller). The friction plates are in contact with the outer surfaces of the side walls. The side walls are attached to the four sides of the intermediate bearing plate and hence move together with it. Screws (A) apply normal forces to the friction interfaces between the friction plates and the side walls. Screws (B) prevent relative movements between the friction and bearing plates. Once the bearing moves, sliding friction forces will be generated at the friction interfaces.

This paper presents the theoretical background of the bearing under base excitation. The acceleration responses of and forces acting on the bearing are derived based on dynamic equilibrium. In addition, the governing equation of horizontal motions, the base shear-horizontal displacement relationship, and conditions for self-centering for the rollers to maintain in contact with the bearing plates and for rolling without sliding, are discussed.

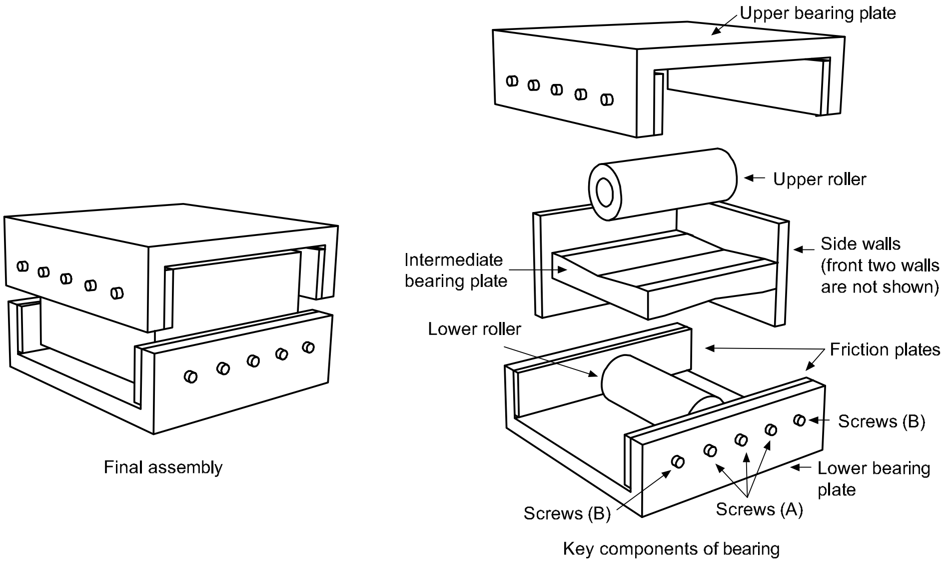

Figure 1 Simplified schematic view of roller seismic isolation bearing

2. ACCELERATIONS AND FORCES UNDER BASE EXCITATION

Acceleration and force responses of the bearing subjected to base excitation along the principal directions, i.e. rolling directions of the rollers, are derived in this section to understand the behavior of the bearing. Since only one roller is mobilized when the bearing moves along each of the two principal directions, only one roller and two bearing plates that sandwich the roller are considered in the derivation. A number of assumptions are made in the derivation: (1) the rollers are in contact with the two bearing plates; (2) the rollers are in pure rolling motion; (3) rolling friction is ignored, since it is typically very small in our application compared to the restoring force and the sliding friction force of the bearing; (4) the lower bearing plate is fixed to a rigid base, and (5) the upper plate is attached to a superstructure that is restrained from rotation. Conditions to maintain the first two assumptions are analytically investigated in later sections.

Figure 2 shows the free body diagram of the two plates and one roller assembly when the roller is on the left side of the lower bearing plate. Note that the sloping angle is exaggerated in the figure for ease of presentation. A horizontal acceleration excitation $\ddot{x}_3$ and a vertical acceleration excitation $\ddot{z}_3$ are imposed to the base of the assembly. For the superstructure, the dynamic equilibrium along the horizontal direction gives

$$m_1\left(\ddot{x}_1+\ddot{x}_3\right)+f_1+f_{Ds}\cos\theta\,\mathrm{sgn}\left(\dot{x}_1\right)=0 \tag{2.1}$$

where m_1 represents the tributary mass carried by the assembly; $\ddot{x}_1$ is the horizontal acceleration response of the superstructure relative to the origin O; f_1 is the static friction force between the roller and the upper bearing plate; f_{Ds} is the sliding friction force produced by the corresponding pair of friction interfaces; θ is the sloping angle; and sgn is a function equal to 1, 0, and -1, if the variable is greater than, equal to, and less than zero, respectively.

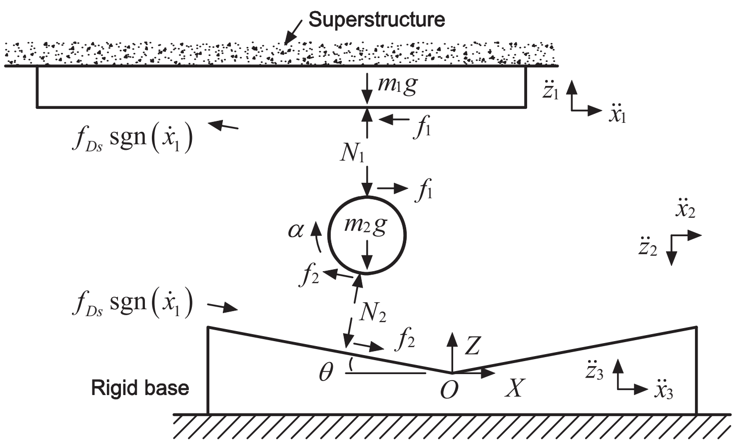

Figure 2 Free body diagram when the roller is on the left

For the vertical direction, we have

$$m_1(\ddot{z}_1+\ddot{z}_3)-N_1+m_1g-f_{Ds}\sin\theta\,\mathrm{sgn}\left(\dot{x}_1\right)=0 \tag{2.2}$$

where $\ddot{z}_1$ is the vertical acceleration response of the superstructure relative to O; N_1 is the normal force between the roller and the upper plate; and g is the acceleration of gravity. The equation of dynamic equilibrium for the roller along the horizontal direction is

$$m_2\left(\ddot{x}_2+\ddot{x}_3\right)-f_1+f_2\cos\theta-N_2\sin\theta=0 \tag{2.3}$$

where m_2 and $\ddot{x}_2$ are the mass and horizontal acceleration response of the roller relative to O, respectively; and f_2 and N_2 are the static friction force and normal force between the roller and the lower bearing plate, respectively. For the vertical direction, we have

$$m_2\left(\ddot{z}_2-\ddot{z}_3\right)-N_1+f_2\sin\theta+N_2\cos\theta-m_2g=0 \tag{2.4}$$

where $\ddot{z}_2$ is the vertical acceleration response of the roller relative to O. The rotational dynamic equilibrium of the roller gives

$$I\alpha-f_1R-f_2R=0 \tag{2.5}$$

where α, I_2 and R are the angular acceleration, moment of inertia and radius of the roller, respectively. If the roller is in a pure rolling motion, compatibility requirements lead to

$$\ddot{x}_2 = R\cos\theta \cdot \alpha \tag{2.6}$$
$$\ddot{z}_2 = R\sin\theta \cdot \alpha \tag{2.7}$$
$$\ddot{x}_1 = \ddot{x}_2 + R\alpha \tag{2.8}$$
$$\ddot{z}_1 = -\ddot{z}_2 \tag{2.9}$$

Rearrange equations (2.1) to (2.9) in a matrix form gives

$$\begin{pmatrix} m_1 & 0 & 0 & 0 & 0 & 1 & 0 & 0 & 0 \\ 0 & m_1 & 0 & 0 & 0 & 0 & 0 & -1 & 0 \\ 0 & 0 & m_2 & 0 & 0 & -1 & \cos\theta & 0 & -\sin\theta \\ 0 & 0 & 0 & m_2 & 0 & 0 & \sin\theta & -1 & \cos\theta \\ 0 & 0 & 0 & 0 & I & -R & -R & 0 & 0 \\ 0 & 0 & 1 & 0 & -R\cos\theta & 0 & 0 & 0 & 0 \\ 0 & 0 & 0 & 1 & -R\sin\theta & 0 & 0 & 0 & 0 \\ 1 & 0 & -1 & 0 & -R & 0 & 0 & 0 & 0 \\ 0 & 1 & 0 & 1 & 0 & 0 & 0 & 0 & 0 \end{pmatrix} \begin{pmatrix} \ddot{x}_1 \\ \ddot{z}_1 \\ \ddot{x}_2 \\ \ddot{z}_2 \\ \alpha \\ f_1 \\ f_2 \\ N_1 \\ N_2 \end{pmatrix} = \begin{pmatrix} -m_1\ddot{x}_3 - f_{Ds}\cos\theta\,\mathrm{sgn}(\dot{x}_1) \\ -m_1(g+\ddot{z}_3) + f_{Ds}\sin\theta\,\mathrm{sgn}(\dot{x}_1) \\ -m_2\ddot{x}_3 \\ m_2(g+\ddot{z}_3) \\ 0 \\ 0 \\ 0 \\ 0 \\ 0 \end{pmatrix}$$

By solving the system of linear equations, we have, for example, the acceleration response of the superstructure

$$\ddot{x}_1 = \frac{2R^2\cos^2\frac{\theta}{2}\left\{f_{Ds}\,\mathrm{sgn}(\dot{x}_1) + m_1\ddot{x}_3 + \left[f_{Ds}\,\mathrm{sgn}(\dot{x}_1) + (m_1+m_2)\ddot{x}_3\right]\cos\theta - (\ddot{z}_3+g)(m_1+m_2)\sin\theta\right\}}{I + (2m_1+m_2)R^2 + 2m_1R^2\cos\theta}$$

Since the mass of the superstructure m_1 is much larger than the mass of the roller m_2, dividing both the denominator and numerator by m_1 and ignoring m_2/m_1 leads to

$$\ddot{x}_1 = \frac{-\cos^2\frac{\theta}{2}\left\{(1+\cos\theta)\left[\ddot{x}_3 + f_{Ds}/m_1\,\mathrm{sgn}(\dot{x}_1)\right] - (\ddot{z}_3+g)\sin\theta\right\}}{1+\cos\theta}$$

further simplification leads to

$$\ddot{x}_1 = -\cos^2\frac{\theta}{2}\left[\ddot{x}_3 + f_{Ds}/m_1\,\mathrm{sgn}(\dot{x}_1)\right] + \frac{1}{2}\sin\theta(\ddot{z}_3+g)$$

In a similar manner, the solutions for all the variables are

$$\begin{pmatrix} \ddot{x}_1 \\ \ddot{z}_1 \\ \ddot{x}_2 \\ \ddot{z}_2 \\ \alpha \\ f_1 \\ f_2 \\ N_1 \\ N_2 \end{pmatrix} \approx \begin{pmatrix} -\cos^2\frac{\theta}{2}\left[\ddot{x}_3 + f_{Ds}/m_1 \operatorname{sgn}(\dot{x}_1)\right] + \frac{1}{2}\sin\theta(\ddot{z}_3 + g) \\ \frac{1}{2}\sin\theta\left[\ddot{x}_3 + f_{Ds}/m_1 \operatorname{sgn}(\dot{x}_1)\right] - \sin^2\frac{\theta}{2}(\ddot{z}_3 + g) \\ \frac{1}{2}\cos\theta\left\{-\left[\ddot{x}_3 + f_{Ds}/m_1 \operatorname{sgn}(\dot{x}_1)\right] + \tan\frac{\theta}{2}(\ddot{z}_3 + g)\right\} \\ \frac{1}{2}\sin\theta\left\{-\left[\ddot{x}_3 + f_{Ds}/m_1 \operatorname{sgn}(\dot{x}_1)\right] + \tan\frac{\theta}{2}(\ddot{z}_3 + g)\right\} \\ \frac{1}{2R}\left\{-\left[\ddot{x}_3 + f_{Ds}/m_1 \operatorname{sgn}(\dot{x}_1)\right] + \tan\frac{\theta}{2}(\ddot{z}_3 + g)\right\} \\ -m_1\left\{\sin^2\frac{\theta}{2}\left[\ddot{x}_3 + f_{Ds}/m_1 \operatorname{sgn}(\dot{x}_1)\right] + \frac{1}{2}\sin\theta(\ddot{z}_3 + g)\right\} \\ m_1\left\{\sin^2\frac{\theta}{2}\left[\ddot{x}_3 + f_{Ds}/m_1 \operatorname{sgn}(\dot{x}_1)\right] + \frac{1}{2}\sin\theta(\ddot{z}_3 + g)\right\} \\ m_1\left\{\frac{1}{2}\sin\theta\left[\ddot{x}_3 + f_{Ds}/m_1 \operatorname{sgn}(\dot{x}_1)\right] + \cos^2\frac{\theta}{2}(\ddot{z}_3 + g)\right\} \\ m_1\left\{\frac{1}{2}\sin\theta\left[\ddot{x}_3 + f_{Ds}/m_1 \operatorname{sgn}(\dot{x}_1)\right] + \cos^2\frac{\theta}{2}(\ddot{z}_3 + g)\right\} \end{pmatrix}$$

When the roller is on the right side of the center of the lower bearing plate, the free body diagram is shown in Figure 3.

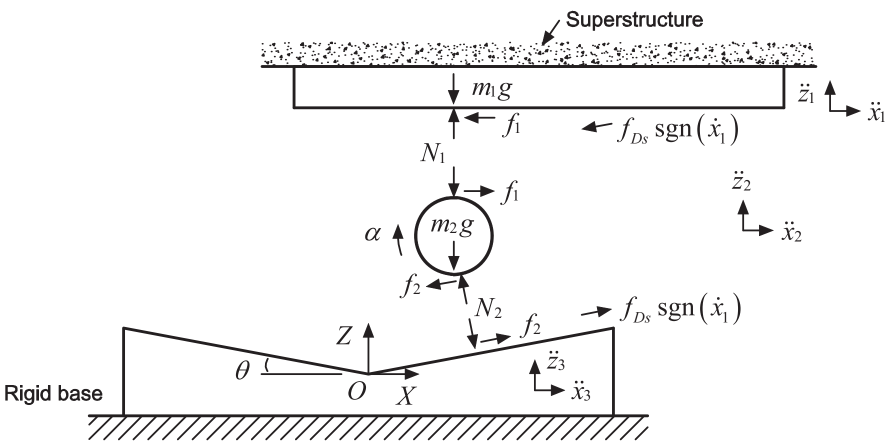

Figure 3 Free body diagram when the roller is on the right

The matrix form for the equations of dynamic equilibrium is

$$\begin{pmatrix} m_1 & 0 & 0 & 0 & 0 & 1 & 0 & 0 & 0 \\ 0 & m_1 & 0 & 0 & 0 & 0 & 0 & -1 & 0 \\ 0 & 0 & m_2 & 0 & 0 & -1 & \cos\theta & 0 & \sin\theta \\ 0 & 0 & 0 & -m_2 & 0 & 0 & -\sin\theta & -1 & \cos\theta \\ 0 & 0 & 0 & 0 & I & -R & -R & 0 & 0 \\ 0 & 0 & 1 & 0 & -R\cos\theta & 0 & 0 & 0 & 0 \\ 0 & 0 & 0 & 1 & -R\sin\theta & 0 & 0 & 0 & 0 \\ 1 & 0 & -1 & 0 & -R & 0 & 0 & 0 & 0 \\ 0 & 1 & 0 & -1 & 0 & 0 & 0 & 0 & 0 \end{pmatrix} \begin{pmatrix} \ddot{x}_1 \\ \ddot{z}_1 \\ \ddot{x}_2 \\ \ddot{z}_2 \\ \alpha \\ f_1 \\ f_2 \\ N_1 \\ N_2 \end{pmatrix} = \begin{pmatrix} -m_1\ddot{x}_3 - f_{Ds}\cos\theta\,\mathrm{sgn}(\dot{x}_1) \\ -m_1(g+\ddot{z}_3) - f_{Ds}\sin\theta\,\mathrm{sgn}(\dot{x}_1) \\ -m_2\ddot{x}_3 \\ m_2(g+\ddot{z}_3) \\ 0 \\ 0 \\ 0 \\ 0 \\ 0 \end{pmatrix}$$

Complete solutions that includes both conditions when the roller is on the left and right sides of the lower bearing plate are

$$\ddot{x}_1 = -\cos^2\frac{\theta}{2}\left[\ddot{x}_3 + f_{Ds}/m_1\,\mathrm{sgn}(\dot{x}_1)\right] - \frac{1}{2}\sin\theta(\ddot{z}_3+g)\mathrm{sgn}(x_1) \tag{2.10}$$

$$\ddot{z}_1 = -\frac{1}{2}\sin\theta\left[\ddot{x}_3 + f_{Ds}/m_1\,\mathrm{sgn}(\dot{x}_1)\right]\mathrm{sgn}(x_1) - \sin^2\frac{\theta}{2}(\ddot{z}_3+g) \tag{2.11}$$

$$\ddot{x}_2 = -\frac{1}{2}\cos\theta\left\{\left[\ddot{x}_3 + f_{Ds}/m_1\,\mathrm{sgn}(\dot{x}_1)\right] + \tan\frac{\theta}{2}(\ddot{z}_3+g)\mathrm{sgn}(x_1)\right\} \tag{2.12}$$

$$\ddot{z}_2 = -\frac{1}{2}\sin\theta\left\{\left[\ddot{x}_3 + f_{Ds}/m_1\,\mathrm{sgn}(\dot{x}_1)\right] + \tan\frac{\theta}{2}(\ddot{z}_3+g)\mathrm{sgn}(x_1)\right\} \tag{2.13}$$

$$\alpha = -\frac{1}{2R}\left\{\left[\ddot{x}_3 + f_{Ds}/m_1\,\mathrm{sgn}(\dot{x}_1)\right] + \tan\frac{\theta}{2}(\ddot{z}_3+g)\mathrm{sgn}(x_1)\right\} \tag{2.14}$$

$$f_1 = -f_2 = m_1\left\{-\sin^2\frac{\theta}{2}\left[\ddot{x}_3 + f_{Ds}/m_1\,\mathrm{sgn}(\dot{x}_1)\right] + \frac{1}{2}\sin\theta(\ddot{z}_3+g)\mathrm{sgn}(x_1)\right\} \tag{2.15}$$

$$N_1 = N_2 = m_1\left\{-\frac{1}{2}\sin\theta\left[\ddot{x}_3 + f_{Ds}/m_1\,\mathrm{sgn}(\dot{x}_1)\right]\mathrm{sgn}(x_1) + \cos^2\frac{\theta}{2}(\ddot{z}_3+g)\right\} \tag{2.16}$$

3. GOVERNING EQUATION OF HORIZONTAL MOTIONS

Equation (2.10) is of great interest since it represents the governing equation of horizontal motions of the bearing (superstructure of the bridge). In our applications, a small sloping angle θ is typically used. Thus, $\cos^2\theta/2 \approx 1$. Simplifying and re-arranging equation(2.10), and multiplying both sides of the equation by m_1 lead to

$$m_1\ddot{x}_1 + \frac{1}{2}m_1\sin\theta(\ddot{z}_3+g)\mathrm{sgn}(x_1) + f_{Ds}\,\mathrm{sgn}(\dot{x}_1) = -m\ddot{x}_3 \tag{3.1}$$

The second term of equation (3.1) represents the restoring force f_S of the bearing. The equation can also be expressed as

$$m_1\ddot{x}_1 + f_S\,\mathrm{sgn}(x_1) + f_{Ds}\,\mathrm{sgn}(\dot{x}_1) = -m_1\ddot{x}_3 \tag{3.2}$$

where

$$f_S = \frac{1}{2} m_1 \left(\ddot{z}_3 + g \right) \sin\theta \tag{3.3}$$

Based on equation (3.2), it can be seen that the maximum base shear V_p along the principal direction of the bearing is

$$V_p = f_S + f_{Ds} \tag{3.4}$$

It is clear that from equations (3.3) and (3.4) that the base shear is independent of the magnitude and frequency content of the horizontal base acceleration $\ddot{x}_3$. This reduces the possibility of resonance between the bearing and base excitation.

If both the upper and lower rollers of the bearing are mobilized, the resultant base shear will be $\sqrt{2}$ times the base shear along the principal directions, that is,

$$V_{\max} = \sqrt{2} f_S + \sqrt{2} f_{Ds} = \sqrt{2}\, V_p \tag{3.5}$$

This force should be considered in the design of the bridge substructure on which the bearing is seated. Figure 4 schematically illustrates the base shear-horizontal displacements relationship of the bearing along the principal directions.

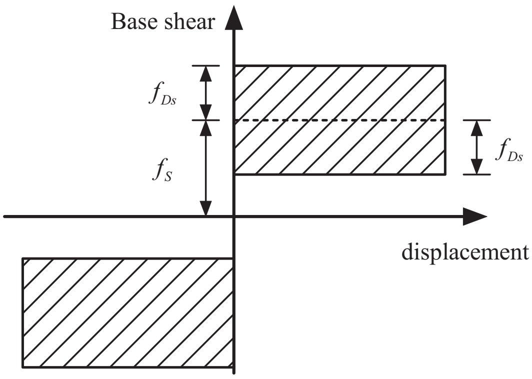

Figure 4 Base shear versus horizontal displacements

Note that for a pure rolling motion, the relative displacement of the superstructure x_1 is twice that of the roller x_2 as shown in Figure 5, that is,

$$2x_2 = x_1 \tag{3.6}$$

This means the displacement capacity of a bridge superstructure seated on a roller bearing is twice the available travel that can be provided by the bearing plate to the roller. This is advantageous, particularly when large displacement capacity is needed.

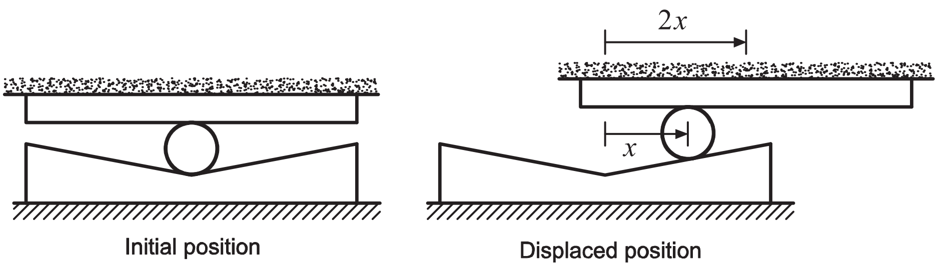

Figure 5 Relationship between displacements of the roller and superstructure

4. CONDITIONS FOR SELF-CENTERING

To maintain self-centering capability of the bearing, the restoring force f_S needs to be larger than the sliding friction force f_{Ds}. AASHTO (2000) requires that the restoring force be greater than or equal to 1.05 times the characteristic strength of the bearing. This means

$$f_S \geq 1.05 f_{Ds} \tag{4.1}$$

Thus, the maximum allowable sliding friction force f_{Dsa} is

$$f_{Dsa} = \frac{f_S}{1.05} \tag{4.2}$$

5. CONDITIONS FOR ROLLERS TO MAINTAIN IN CONTACT WITH BEARING PLATES

For the rollers to maintain in contact with the bearing plates, forces N_1 and N_2 have to be positive, that is

$$N_1 = N_2 = m_1 \left\{ -\frac{1}{2} \sin\theta \left[\ddot{x}_3 + f_{Ds} / m_1 \operatorname{sgn}(\dot{x}_1) \right] \operatorname{sgn}(x_1) + \cos^2 \frac{\theta}{2} (\ddot{z}_3 + g) \right\} > 0 \tag{5.1}$$

When θ is small, the first term of the equation likely becomes small compared to the second term and $\cos^2 \theta / 2 \approx 1$. Thus, equation (5.1) may be simplified and rearranged to equation (5.2), which shows that if the magnitude of the downward vertical base acceleration is smaller than g, the rollers will maintain contact with the bearing plates.

$$\ddot{z}_3 > -g \tag{5.2}$$

If the rollers are not in contact with the bearing plates, the rolling constraint between them does not exist. This means misalignment between the rollers and the bearings plate may happen, causing a permanent displacement when the motion of the bearing stops.

6. CONDITIONS FOR ROLLING WITHOUT SLIDING

Once the static friction force between the roller and the bearing plate f developed by an angular acceleration of the roller exceeds the maximum static friction force f_{st} that can be provided by the contact interface, the roller starts sliding. Once the roller slides, the bearing may exhibit a permanent displacement after earthquakes.

To ensure rolling without sliding, f_{st} must exceed f, that is,

$$f_{st} = \mu_s N_1 \geq |f_1| \text{ and } \mu_s N_2 \geq |f_2| \tag{6.1}$$

Substituting N_1 and f_1 from equations (2.16) and (2.15) into equation (6.1) leads to

$$\mu_s \geq \left| \frac{m_1\left\{-\sin^2\frac{\theta}{2}\left[\ddot{x}_3 + f_{Ds}/m_1 \operatorname{sgn}(\dot{x}_1)\right] + \frac{1}{2}\sin\theta(\ddot{z}_3 + g)\operatorname{sgn}(x_1)\right\}}{m_1\left\{-\frac{1}{2}\sin\theta\left[\ddot{x}_3 + f_{Ds}/m_1 \operatorname{sgn}(\dot{x}_1)\right]\operatorname{sgn}(x_1) + \cos^2\frac{\theta}{2}(\ddot{z}_3 + g)\right\}} \right|$$

Further simplification leads to

$$\mu_s \geq \tan\frac{\theta}{2} \tag{6.2}$$

In a similar manner, substituting N_2 and f_2 from equations (2.16) and (2.15), respectively, into equation (6.1) also leads to equation (6.2). Thus, the sloping angle θ has to satisfy

$$\theta \leq 2\tan^{-1}\mu_s \tag{6.3}$$

This equation shows the upper limit of the sloping angle θ for rolling without sliding increases as the coefficient of static friction μ_s increases. μ_s for steel on steel range from 0.74 for dry conditions to approximately 0.1 for greasy conditions (Avallone and Baumeister, 1996). For a conservative result, μ_s is taken as 0.1. Thus, the condition for rolling without sliding is

$$\theta \leq 11^\circ \tag{6.4}$$

7. CONCLUSIONS

The characteristics of a new roller seismic isolation bearing are presented and discussed. A number of important conclusions are summarized as follows:

(1) The bearing exhibits a maximum base shear independent of the amplitude and frequency content of horizontal ground motions and has a self-centering capability after earthquakes.
(2) The maximum base shear occurs when both the upper and lower rollers are mobilized. The magnitude of the force is the result of the maximum base shears along the principal directions of the bearing.
(3) For the rollers to maintain contact with the bearing plates, the absolute value of the downward acceleration should not exceed approximately one acceleration of gravity.
(4) To prevent sliding of the rollers, the sloping angle of the bearing needs to be smaller than a certain value depending on the coefficient of static friction between the roller and the sloping surface. For steel rollers and steel bearing plates, the upper limit of the sloping angle can be conservatively chosen as 11 degrees.

ACKNOWLEDGEMENT

The authors gratefully acknowledge the Federal Highway Administration for funding the study reported herein (FHWA 094 Project No. DTFH61-98-C00094). They wish to express their sincere appreciation to Philip Yen and James Cooper from FHWA for their support, advice, and encouragement and to Andrew Whittaker and

Michael Constantinou from the University at Buffalo for their valuable comments in the development of the bearing.

REFERENCES

AASHTO. (2000). Guide specifications for seismic isolation design, Washington, DC.
Avallone, E.A., and Baumeister, T., III. (1996). Marks' standard handbook for mechanical engineers, 10th Ed., McGraw-Hill, London, U.K.
Constantinou, M. C., Whittaker, A. S., Kalpakidis, Y., Fenz, D. M., and Warn, G. P. (2007). "Performance of seismic isolation hardware under service and seismic loading." Report No. MCEER-07-0012, Multidisciplinary Center for Earthquake Engineering Research, University at Buffalo, State University of New York, Buffalo, NY.
Earthquake Protection Systems, Inc. (2008). "Friction Pendulum seismic isolation bearings." <http://www.earthquakeprotection.com/product2.html>.
Lee, G. C., Liang, Z., and Niu, T.-C. (2005). Seismic isolation bearing, US Patent No. 6971795 B2.
Naeim, F. and Kelly, J.M. (1999). Design of Seismic Isolated Structures, J. Wiley & Sons, New York.
R. J. Watson, Inc. (2008). "The EradiQuake System."
<http://www.rjwatson.com/eqs_bearing.htm>.